Spatial variability and delineation of soil fertility management zones using geostatistics and fuzzy c-means clustering in an irrigated wheat system in alborz province, Iran

Hamed Rezaei†, Leila Esmaeelnejad and Rasoul Mirkhani

Soil and Water Research Institute, Agricultural Research, Education and Extension Organization (AREEO), Karaj, Iran

†Corresponding Author Email: hrezaei@areeo.ac.ir

ABSTRACT

Sustainable soil management and precision nutrient application in irrigated wheat systems require a detailed understanding of the spatial variability of soil properties and their implications for site-specific practices. This study aimed to quantify the spatial variability of some key soil fertility attributes and to delineate soil fertility management zones (MZs) for site-specific nutrient management in irrigated wheat fields of Alborz province, Iran. A total of 222 geo-referenced surface soil samples (0–30 cm) were collected on a 1,650 × 1,650 m grid. Soil pH, electrical conductivity (EC), soil organic carbon (SOC), total neutralizing value (TNV), particle-size distribution, and available macro- and micronutrients (P, K, Ca, Mg, Fe, Mn, Zn, Cu) were determined by the standard laboratory methods. Descriptive statistics and Pearson correlations were computed, and geostatistical analyses (semivariograms and ordinary kriging) were used to characterize and map spatial variability. Principal component analysis (PCA) followed by fuzzy c-means clustering were applied to delineate soil fertility MZs.

Most soil properties exhibited moderate to high coefficients of variation, with only low variability for the pH, while clay and TNV fell into the moderate class and EC, SOC, and most available nutrients showed high variability. Semivariogram modelling indicated exponential and Gaussian models as the best fit for the majority of properties, with moderate to strong spatial dependence and ranges varying from 1.65 to 105.6 km. Kriged maps revealed that about 78% of the area was non-saline (EC <4 dS m^{-1}), whereas roughly 22% was saline, and more than half of the fields had SOC <1%, highlighting significant constraints on yield and soil health. Micronutrient maps showed widespread Zn and Fe deficiencies in the western, more alkaline and lighter-textured parts of the province. PCA identified four principal components explaining 66.6% of the total variance, capturing major gradients in overall fertility, lime–nutrient–texture status, salinity–pH conditions, and macronutrient availability.

Using the first four PCs as input, fuzzy c-means clustering and cluster validity indices (fuzzy performance index and normalized classification entropy) indicated that four MZs provided the most appropriate partitioning of the fields. These MZs differed significantly in SOC, EC, pH, texture, and nutrient status. In zones with high K and P but adequate Fe and Zn, further K and P fertilization is unnecessary, whereas zones with low P, Fe, and Zn and low SOC require targeted P and micronutrient inputs and organic matter management. The delineated MZs and associated maps offer a practical framework for variable-rate fertilization and more efficient soil sampling, supporting sustainable intensification of irrigated wheat production in Alborz province and similar semi-arid regions.

Keywords: Aridisols, delineation of management zones, fertilizer application rate, nutrient management, precision agriculture, wheat production.

How to Cite: Rezaei, H., Esmaeelnejad, L. and Mirkhani, R., 2025. Spatial variability and delineation of soil fertility management zones using geostatistics and fuzzy c-means clustering in an irrigated wheat system in alborz province, Iran. Dryland Soil Res. 2(2), 1–21. https://doi.org/10.47176/dlsr.2.2.1052

1. Introduction

Soils exhibit heterogeneous physical, chemical, and biological properties that vary in both space and time (Bevington et al. 2016). Intrinsic factors such as organisms, parent material, relief, climate, and time, together with extrinsic factors including fertilizer management and irrigation practices, jointly contribute to the spatial variability of soil properties (Denton et al. 2017). Sustainable soil management, precision agriculture, and site-specific crop production require appropriate knowledge of soil properties to maintain or improve soil fertility and thereby reduce soil degradation (Behera et al. 2018). Soil heterogeneity arises from the combined effects of physical, chemical, and biological processes, and individual soil properties often exhibit different degrees of variability (Seyedmohammadi et al. 2018). Spatial and temporal variation in soil properties is a key characteristic of real agroecosystems (Palmer et al. 2017). Effective soil and crop management therefore requires a sound understanding of the spatial patterns of soil properties, so that fertilizer application can be adjusted in a site-specific manner according to soil and crop requirements (Shukla et al. 2017). Geostatistical techniques provide a set of numerical tools for quantifying and predicting soil properties at unsampled locations (Behera et al. 2018; Barrena-González et al. 2023).

The delineation of management zones (MZs) is a practical approach to dealing with spatial variability in soil properties. Management zones are defined as subregions within a field that are relatively homogeneous with respect to soil and crop conditions and therefore warrant distinct management and input levels based on plant requirements and soil characteristics (Behera et al. 2018). In other words, each MZ represents an area that is internally similar in terms of key soil attributes (Barrena-González et al. 2023). Previous studies have delineated soil MZs in paddy fields based on soil fertility using fuzzy clustering methods in Iran and India (Tripathi et al. 2015). Other researchers have combined principal component analysis with fuzzy c-means clustering to delineate MZs for different crops and regions (Shukla et al. 2017; Behera et al. 2018).

Wheat is a strategic crop that occupies a substantial share of agricultural production in many developing countries, yet global wheat production still falls short of meeting the food demand of a growing population. Wheat is also one of the most widely cultivated cereals in Alborz province, Iran. According to statistics from the Ministry of Jihad-e-Agriculture for the 2016–2017 growing season, the mean wheat yield in Alborz province was about 5.3 t ha^{-1}, whereas the maximum recorded yield approached 13 t ha^{-1}. These values are consistent with more recent provincial and national reports indicating average irrigated wheat yields of approximately 5–5.2 t ha^{-1} and yields of up to about 12–14 t ha^{-1} for high-performing farmers in Alborz. This substantial yield gap highlights considerable potential for yield improvement through better farm management, including the delineation of MZs to guide the site-specific application of agricultural inputs.

Among the various factors influencing wheat yield, nutrient supply plays a pivotal role. Balanced fertilization is essential to achieve optimal wheat yields, and the deficiency of a single nutrient or imbalanced ratios such as N/K can constrain crop performance. It is also critical to maintain the availability of each nutrient at levels commensurate with crop demand (Behera et al. 2018). Nutrient-related yield limitations are inherently site-specific because nutrient availability is strongly governed by soil properties. The quality of organic amendments and their C:N ratio should also be considered when assessing their possible role in soil nutrient management. Doetterl et al. (2025) reported that soil organic carbon (SOC) and soil pH modify soil chemical conditions and thereby influence nutrient availability. Consequently, assessment of soil properties is fundamental for improving nutrient management and soil fertility, and fertilizer recommendations should ideally be based on soil test results for instance organic processes that take place during the breakdown of organic material can also affect the conversion of organic material and nutrient availability in agriculture.

However, conventional soil testing is costly, and many farmers cannot afford detailed analyses. In this context, MZs can serve as a generalized form of soil testing at a broader spatial scale, providing a practical tool for farmers and extension specialists to improve soil fertility management.

In Alborz province, diverse soil management practices and variable fertilizer application rates are expected to generate pronounced spatial variability in soil properties. Moreover, existing information on spatially variable soil attributes and MZs in the region is limited and fragmented. Uniform nutrient recommendations may therefore lead to inappropriate fertilization, causing both over- and under-application of nutrients within and among fields. In light of these considerations, the present study was conducted (i) to evaluate the spatial variability of soil properties and (ii) to delineate MZs in irrigated wheat fields of Alborz province using a combination of statistical and geostatistical techniques.

2. Materials and Methods

2.1. Study area

Agricultural lands of Alborz province, Iran, were considered as the study area (Figure 1). The region has an arid to semi-arid cold climate with a mean annual rainfall of 247.3 mm (Alborz Meteorological Office, 2026). Most of the rainfall occurs between October and May. The mean maximum and minimum temperatures are 34.6 °C and −2.9 °C, typically recorded in July and February, respectively. The dominant soil orders in the study area

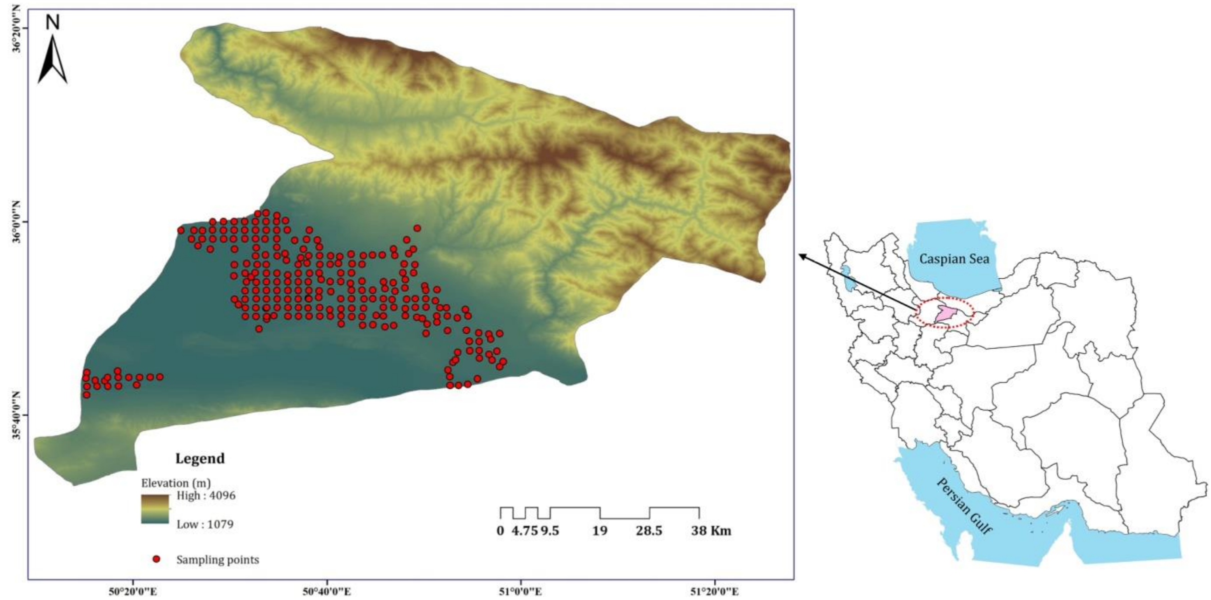

Fig. 1. Location of the study area (Alborz province, Iran) with sampling points.

are Entisols, Inceptisols, and Aridisols (Soil Survey Staff, 2026), encompassing a wide range of texture classes. Wheat is cultivated as an irrigated crop throughout much of the agricultural land in this province.

2.2. Soil sampling, processing and analysis

sing the land-use map of Alborz province and a 1,650 × 1,650 m grid, 222 sampling locations were selected (Figure 1). At each location, surface soil samples (0–30 cm) were collected using a hand auger. A composite sample was obtained at each site by mixing five subsamples. After air-drying, grinding, and passing through a 2 mm sieve, soil pH, soil organic carbon (SOC), available phosphorus (AP), available potassium (AK), available Ca, Mg, Fe, Mn, Zn, Cu, and particle size distribution were determined. Soil pH was measured in a 1:1 (w/w) soil–water suspension. Organic carbon was determined by the Walkley–Black wet oxidation method (Walkley and Black 1934). Available P was measured using the Olsen method (Olsen et al. 1954), and available K by the method of Hanway and Heidel (1952). Available Ca, Mg, Fe, Mn, Zn, and Cu were also measured, and particle size distribution was determined using the hydrometer method (Gee and Bauder 1986).

2.3. Statistical and geostatistical analysis

Statistical analysis

All statistical analyses were performed using SPSS version 28.0 (SPSS Inc., Chicago, IL, 2025). Descriptive statistics were first calculated for all soil properties. The Kolmogorov–Smirnov (K–S) test was used to assess the normality of the distributions. Pearson's correlation coefficients were computed to examine relationships among soil properties.

2.4. Geostatistical analysis

Geostatistical analyses were conducted using GS+ version 10.2 for Windows (Gamma Design, Inc., 2026). Experimental semivariograms were computed for each soil property according to Equation (1):

$$\gamma_h = \frac{1}{2N(h)} \sum_{\alpha=1}^{N(h)} \left[Z(X_a) - Z(X_a + h) \right]^2 \qquad [1]$$

Where $\gamma(h)$ is the semivariance, $N(h)$ is the number of sample pairs separated by the lag distance h, $Z(X_\alpha)$ is the measured value of the soil property at location X_α , and $Z(X_\alpha+h)$ is the corresponding value at a distance h from that location. Different theoretical semivariogram models, including Gaussian, exponential, and spherical models (Equations 2, 3, and 4, respectively), were fitted to the experimental semivariograms to identify the best-fit model for each soil property (Burgess and Webster, 1980).

$$\gamma(h) = C_0 + C_1 \left[1 - \exp\left(-\frac{h^2}{a^2} \right) \right] \qquad [2]$$

$$\gamma(h) = C_0 + C_1 \left[1 - \exp\left(-\frac{h}{a} \right) \right] \qquad [3]$$

$$\begin{cases} \gamma(h) = C_0 + C_1 \left[\dfrac{3h}{2a} - \dfrac{h^3}{2a^3} \right] & \text{when } h \le a \\ \gamma(h) = C_0 + C_1 & \text{when } h > a \end{cases} \qquad [4]$$

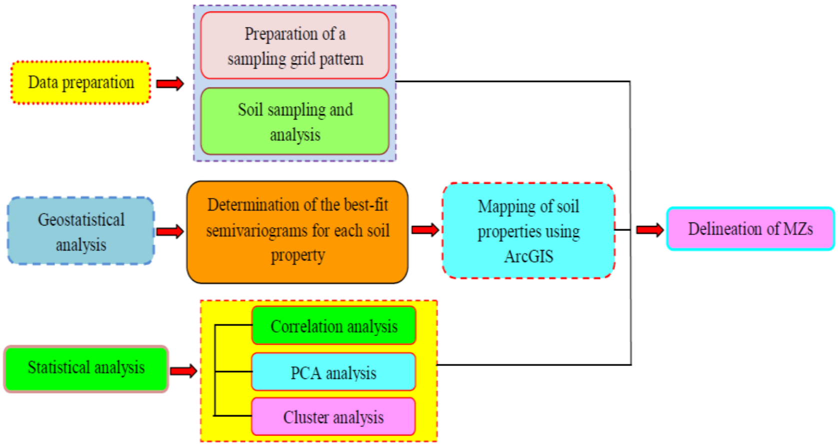

Fig. 2. Flowchart of data processing.

Where C_0, C_1 and a, is the nugget, the partial sill, and the range of spatial dependence to reach the sill ($C_0 + C_1$), respectively. Cambardella et al. (1994), introduced a measure for spatial dependence determination ($DSD = C_0/(C_0+C_1)\times 100$) with three classes including strong, moderate, and weak when DSD < 25%; 25 < DSD ≤ 75%; and DSD > 75%, respectively.

Li et al. (2025) used the coefficient of determination (R^2) (Equation 5) and also Behera et al. (2018) applied mean square error (MSE) (Equation 6) for Selection of best fitted semivariograms:

$$R^2 = 1 - \left[\left(\sum_{i=1}^{n}(O_i - P_i)^2\right) \Big/ \left(\sum_{i=1}^{n}(O_i - \bar{O}_i)^2\right)\right] \quad [5]$$

$$MSE = \frac{\sum_{i=1}^{n}(O_i - P_i)^2}{n} \quad [6]$$

Where, n is the number of observation for each case, O_i the measured value of soil parameter, $\bar{O}_i$ the average of measured value and P_i the predicted value.

Ordinary kriging (OK) using fitted semivariogram models applied for estimation of various soil properties at un-sampled sites (Shi et al., 2024; Stirling et al., 2023). Mappings were done with Arc GIS 10.4.1.

The analogies of the interpolated maps validities were judged by the goodness-of- prediction criterion (G) as Equation 7 (Agterberg 1984):

$$G = 1 - \frac{MSE}{MSE_{average}} \times 100 \quad [7]$$

Where, $MSE_{average}$ is the mean square error obtained from a catchment average value as an estimate for all test data (using exploratory statistics). Positive G values (G > 0), implies that the interpolated map is more valid than the area average and vice versa (Parfitt et al. 2009).

2.5. Principal component analysis

Principal component analysis (PCA) is used to shrink dimension and provide new variables named principal components (PCs) (Behera et al. 2018). For this purpose, a correlation matrix is needed to be developed using soil properties as inputs. After running PCA procedure, generated PCs with Eigen values ≥ 1.0 were selected to develop the management zone classes.

2.6. Fuzzy clustering algorithm

Fuzzy *k*-means (FKM) was used to group the dataset into two to seven clusters by using FuzME software (Minasny and McBratney 2006). Two important factors including Fuzzy performance index (FPI, (Equation 8) and normalized classification entropy (NCE, (Equation 9) were used to get optimal and suitable number of clusters (Behera et al. 2018). FPI almost is used to determine the level of membership sharing of different classes or in the other words implies the degree of fuzziness. NCE is applied to determine the best number of clusters for designation of management zones (Wang et al., 2026).

$$FPI = 1 - S\frac{C}{C-1}\left[1 - \frac{\sum_{i=1}^{c}\sum_{k=1}^{n}(\mu ik)^2}{n}\right] \quad [8]$$

$$NCE = \frac{n}{n-c}\left[1 - \frac{\sum_{k=1}^{n}\sum_{i=1}^{n}\mu_{ik}\log_a(\mu_{ik})}{n}\right] \quad [9]$$

Where, c, n, μ_{ik} and log_a indicate number of cluster, number of observations, fuzzy membership and natural logarithm, respectively. The lowest values of FPI and NCE determined the optimal cluster numbers. The differences among the finally delineated MZs were tested by variance analysis. A flowchart of data processing procedure is shown in Figure 2.

Table 1. Descriptive statistical parameters of soil properties of the study area.

Soil properties		min	max	mean	SD	CV(%)	Skewness	Kurtosis
SOC (%)	%	0.07	3.53	0.94	0.53	56.4	1.8*	5.77
TNV (%)		4.1	23.2	12.85	4.5	35.02	0.25	-0.77
K	mg kg^{-1}	86	800	342.6	143.7	41.9	0.465	-0.19
P		1.2	75	17.08	16.48	96.5	1.56*	1.81
Mg_{ava}		88	1275	434.1	221	50.91	1.19*	2.01
Fe_{ava}		1.2	54.7	5.94	5.83	98.15	6.45*	52.75
Mn_{ava}		1.43	28.2	10.64	5.25	49.3	0.648	0.45
Zn_{ava}		0.14	4.62	1.2	0.93	49	1.65*	2.51
Cu_{ava}		0.2	7	1.82	1.09	59.89	1.89*	6.33
pH	-	7.3	8.7	7.83	0.21	2.68	0.463	2.49
EC	dS m^{-1}	0.59	15.39	3.06	2.96	97	2.19*	4.49
Sand	%	10	82	39.86	19.4	48.7	0.39	-0.93
Silt		5	55	33.81	12.8	37.86	-0.35	-0.99
Clay		10	48	26.33	8.6	32.66	0.21	-0.34

EC: electrical conductivity; SOC: soil organic carbon; P_{ava}: available phosphorous; K_{ava}: available potassium; Mg_{ava}: exchangeable magnesium; Fe_{ava}: available Ferrous; Mn_{ava}: available manganese; Zn_{ava}: available Zinc; Cu_{ava}: available Copper; SD: standard deviation; CV: coefficient of variation; TNV: total neutralizing value.* means skewness > 1 and these parameters need normalization.

3. Results

3.1. Characteristic and variability of soil properties

The studied soil properties showed wide variation across the sampling sites (Table 1). The mean values of soil pH, electrical conductivity (EC), and soil organic carbon (SOC) were 7.83 ± 0.21 (range 7.3–8.7), 3.06 ± 2.96 dS m^{-1} (range 0.59–15.39 dS m^{-1}), and 0.94 ± 0.53% (range 0.07–3.53%), respectively. The mean concentrations of available K, P, Mg, Fe, Mn, Zn, and Cu were 342.6 ± 143.7 mg kg^{-1} (range 86–800 mg kg^{-1}), 17.08 ± 16.48 mg kg^{-1} (range 1.4–75 mg kg^{-1}), 434.1 ± 221 mg kg^{-1} (range 88–1275 mg kg^{-1}), 5.94 ± 5.83 mg kg^{-1} (range 1.2–54.7 mg kg^{-1}), 10.64 ± 5.25 mg kg^{-1} (range 1.43–28.2 mg kg^{-1}), 1.20 ± 0.93 mg kg^{-1} (range 0.14–4.62 mg kg^{-1}), and 1.82 ± 1.09 mg kg^{-1} (range 0.20–7.00 mg kg^{-1}), respectively. The mean values of total neutralizing value (TNV), sand, silt, and clay were 12.85% (range 4.1–23.3%), 39.86% (range 10–82%), 33.82% (range 5–55%), and 26.33% (range 10–48%), respectively. Several soil properties, including SOC, available P, Mg, Fe, Zn, Cu, and EC, exhibited significant positive skewness; therefore, these variables were log-transformed prior to geostatistical analysis to approximate normality.

"The degree of spatial dependence (DSD) provides further insights into the driving factors of soil variability. Properties exhibiting strong spatial dependence, such as pH, EC, and TNV, are primarily governed by intrinsic pedogenic factors, including parent material mineralogy and regional climate. Conversely, the moderate spatial dependence observed for available nutrients (e.g., P, K, Zn, Cu) indicates a mixed influence of both intrinsic soil properties and extrinsic anthropogenic factors, notably the varying rates of inorganic fertilizer applications and tillage practices across different farms."

3.2. Relationships among different soil properties

The Pearson's correlation coefficients describing relationships among the studied soil properties are presented in Table 2. Soil properties exhibited both positive and negative correlations, which may reflect similar or contrasting spatial patterns, respectively. Soil organic carbon (SOC) was positively correlated with TNV and with the available forms of K, P, Mg, Fe, Mn, Zn, and Cu, but negatively correlated with sand content. As a key soil attribute, SOC influences major soil functions, including physical, chemical, and biological processes, and thereby plays a critical role in regulating nutrient availability to crops (Behera et al. 2018).

The content of TNV had a positive correlation with available K, Mg, pH, and clay content, and a negative correlation with available Mn and sand. Available K was positively correlated with available P, Mg, Zn, Cu, and silt and clay contents, but negatively correlated with sand. Available P was positively correlated with Fe, Mn, Zn, Cu, and clay. Available Ca was positively correlated only with EC, whereas available Mg was positively correlated with Fe, Cu, pH, silt, and clay, and negatively correlated with sand.

Available Fe was positively correlated with Mn, Zn, Cu, silt, and clay, and negatively correlated with EC and sand. Available Mn showed positive correlations with Zn, Cu, and EC, and a negative correlation with pH. Available Cu was positively correlated with clay. Soil pH was negatively correlated with EC. In accordance with these

Table 2. Pearson's correlation coefficient values showing relationship among soil properties of the study area.

variable	SOC	TNV	K_{ava}	P_{ava}	Ca_{ava}	Mg_{ava}	Fe_{ava}	Mn_{ava}	Zn_{ava}	Cu_{ava}	pH	EC	sand	silt	clay
SOC	1														
TNV	0.25^{**}	1													
K_{ava}	0.39^{**}	0.24^{**}	1												
P_{ava}	0.49^{**}	0.04	0.3^{**}	1											
Ca_{ava}	0.013	0.001	-0.69	-0.048	1										
Mg_{ava}	0.44^{**}	0.49^{**}	0.32^{**}	0.079	-0.15	1									
Fe_{ava}	0.24^{**}	0.05	0.115	0.157^{*}	-0.14	0.228^{**}	1								
Mn_{ava}	0.28^{**}	-0.14^{*}	0.09	0.172^{*}	-0.06	0.013	0.223^{**}	1							
Zn_{ava}	0.49^{**}	-0.06	0.25^{**}	0.61^{**}	-0.06	-0.039	0.365^{**}	0.286^{**}	1						
Cu_{ava}	0.423^{**}	-0.21	0.26^{**}	0.27^{**}	-0.06	0.261^{**}	0.662^{**}	0.269^{**}	0.449^{**}	1					
pH_{ava}	-0.09	0.27^{**}	0.12	-0.127	-0.33	0.262^{**}	0.08	-0.29^{**}	-0.27^{**}	-0.104	1				
EC	-0.05	-0.05	0.02	0.004	0.25^{**}	-0.004	-0.19^{**}	0.209^{**}	0.056	-0.09	-0.37^{**}	1			
Sand	-0.51^{**}	-0.2^{**}	-0.29^{**}	-0.11	-0.12	-0.53^{**}	-0.18^{**}	-0.15^{*}	-0.137^{*}	-0.49^{**}	0.008	0.166^{*}	1		
Silt	0.4	0.01	0.18^{**}	0.045	0.11	0.301^{**}	0.148^{*}	0.198^{**}	0.168^{*}	0.429^{**}	-0.08	-0.19^{**}	-0.89^{**}	1	
clay	0.47	0.44^{**}	0.35^{**}	0.165^{*}	0.08	0.634^{**}	0.157^{*}	0.043	0.046	0.396^{**}	0.094	-0.077	-0.79^{**}	0.42^{**}	1

**: Correlation is significant at the 0.01 level (2-tailed). *: Correlation is significant at the 0.05 level (2-tailed).
EC: electrical conductivity; SOC: soil organic carbon; P_{ava}: available phosphorous; K_{ava}: available potassium; Mg_{ava}: exchangeable magnesium; Fe_{ava}: available Ferrous; Mn_{ava}: available manganese; Zn_{ava}: available Zinc; Cu_{ava}: available Copper; TNV: total neutralizing value;

findings, Behera et al. (2018) also reported a negative relationship between soil pH and EC. Soil EC was positively correlated with available Ca and Mn and negatively correlated with Fe and pH, consistent with observations by Peralta and Costa (2013), who found that EC was associated with available Ca and Mn. Similarly, Behera and Shukla (2015) reported positive correlations of soil pH and SOC with K, Ca, and Mg, as well as among K, Ca, and Mg, in cropped acid soils of India. The pronounced spatial variability of soil properties, particularly EC and pH, cannot be solely attributed to inherent parent material but is strongly driven by pedogenic processes characteristic of semi-arid environments. In such regions, high evapotranspiration rates coupled with insufficient precipitation limit the leaching of basic cations, leading to secondary salinization and the accumulation of carbonates in the soil profile (Zádorová et al., 2025; Doetterl et al., 2025). The negative correlation observed between pH and EC is a typical pedogenic signature in Aridisols, where the precipitation of calcium carbonates buffers pH while soluble salts remain mobile and concentrate in depressions or poorly drained zones under long-term agricultural irrigation (Stirling et al., 2023). Furthermore, the spatial dependence of SOC is largely governed by historical land use rather than pedogenesis. High SOC variability highlights the influence of spatially non-uniform anthropogenic inputs, such as uneven manure application and crop residue retention, which override the relatively uniform natural biogeochemical carbon cycling in these landscapes.

Beyond natural soil-forming processes, agricultural management practices exert a dominant control over the spatial patterns of soil nutrients. The positive spatial correlations among SOC and available micronutrients (Fe, Zn, Cu, Mn) reflect the critical role of organic matter in forming organo-metallic chelates, which protect these micronutrients from precipitation in calcareous environments (Barrena-González et al., 2023). However, the high spatial variability of P and K indicates a history of non-uniform fertilization strategies. For instance, the accumulation of P in specific zones is a direct consequence of its low mobility in calcareous soils (high TNV) and repeated application of diammonium phosphate exceeding crop removal rates. Conversely, areas showing deficiencies in Fe and Zn, particularly in lighter-textured sandy zones, are likely the result of intensive leaching and poor inherent buffering capacity, emphasizing the need for zone-specific precision agriculture interventions (Shi et al., 2024; Zhang et al., 2026).

3.3. Spatial variability analysis

The semivariogram parameters for the studied soil properties are summarized in Table 3 and illustrated in Figure 3. The Gaussian model provided the best fit for EC, and for the available forms of Cu, Zn, P, as well as for silt. The remaining soil properties were best described by the exponential model. These findings are broadly consistent with previous studies: Davatgar et al. (2012) reported an exponential model as the best fit for available K, and Behera et al. (2018) identified exponential models for available K, Ca, and Mg. In contrast, Behera et al. (2018)

Table 3. Semi-variogram models for soil nutrients and inherent fertility potential properties in the study area.

variable	model	nugget	sill	DSD	SDC	Range (m)	R^2	RSS
S.O.C	Exponential	0.07	0.21	0.498	moderate	3600	0.89	1.19×10^{-3}
T.N.V	Exponential	0.075	0.6	0.125	strong	9400	0.85	0.034
K_{ava}	Exponential	0.117	0.21	0.557	moderate	5400	0.915	5.5×10^{-4}
P_{ava}	Gausian	0.63	0.9	0.7	moderate	7800	0.917	9.9×10^{-3}
Ca_{ava}	Exponential	0.03	0.099	0.307	moderate	2700	0.918	2.37×10^{-4}
Mg_{ava}	Exponential	0.1	0.234	0.427	moderate	7010	0.973	4.2×10^{-4}
Fe_{ava}	Exponential	0.138	0.21	0.657	moderate	5000	0.926	2.55×10^{-4}
Mn_{ava}	Exponential	8	18.5	0.432	moderate	1650	0.853	3.27
Zn_{ava}	Gausian	0.305	0.485	0.629	moderate	6280	0.981	7.35×10^{-4}
Cu_{ava}	Gausian	0.17	0.25	0.68	moderate	4800	0.72	2.29×10^{-3}
pH	Exponential	0.009	0.037	0.241	strong	2400	0.87	4.3×10^{-5}
EC	Gausian	0.41	2.84	0.146	strong	105600	0.987	2.11×10^{-3}
Sand	Exponential	0.07	0.285	0.246	strong	2800	0.938	1.28×10^{-3}
Silt	Gausian	75.1	130	0.578	moderate	3200	0.91	371
clay	Exponential	0.03	0.142	0.211	strong	1700	0.951	2.54×10^{-4}

EC: electrical conductivity; SOC: soil organic carbon; P_{ava}: available phosphorous; K_{ava}: available potassium; Mg_{ava}: exchangeable magnesium; Fe_{ava}: available Ferrous; Mn_{ava}: available manganese; Zn_{ava}: available Zinc; Cu_{ava}: available Copper; TNV: total neutralizing value; DSD: degree of spatial dependence; SDC: spatial dependency classes; RSS: residual sum of squars.

also reported circular, K-Bessel, and exponential models as best fits for pH, SOC, and available K, while Wani et al. (2016) found that the spherical model best described the spatial structure of EC and available P and S. Similarly, Behera et al. (2018) reported exponential models for soil P, Ca, and Mg, and Ferreira et al. (2015) showed that exponential semivariogram models best fitted soil EC and organic matter in olive orchards in Portugal.

3.4. Spatial interpolations of soil properties

Ordinary kriging (OK) was used to interpolate the spatial distribution of soil properties and to generate continuous prediction maps. This approach has also been widely applied in previous studies to assess the spatial variability of soil attributes in different agroecosystems, including oil palm plantations in southern India and croplands in southeastern Córdoba province, Argentina (Behera et al. 2018; Peralta and Costa 2013). The accuracy of the kriged maps was evaluated using two criteria, namely the G statistic and the mean square error (MSE) (Table 4). Lower MSE values indicate that the predicted values are closer to the observed values. In this study, G values ranged from 0.498 to 0.823, which is comparable to those reported by Behera et al. (2018) for similar applications of ordinary kriging in soil studies.

Table 4. Accuracy criteria of the kriged maps of the studied soil properties.

variable	MSE	G(%)
S.O.C	39.38	0.582
T.N.V	30.21	0.721
K_{ava}	0.012	0.823
P_{ava}	3.901	0.801
Ca_{ava}	31.28	0.652
Mg_{ava}	50.21	0.498
Fe_{ava}	26.21	0.736
Mn_{ava}	36.59	0.698
Zn_{ava}	44.56	0.553
Cu_{ava}	42.29	0.611
pH	23.32	0.759
EC	1.15	0.816
Sand	12.25	0.796
Silt	22.12	0.789
clay	3.25	0.812

EC: Electrical Conductivity; SOC: Soil Organic Carbon; P_{ava}: available phosphorous; K_{ava}: available potassium; Mg_{ava}: exchangeable magnesium; Fe_{ava}: available Ferrous; Mn_{ava}: available manganese; Zn_{ava}: available Zinc; Cu_{ava}: available Copper; TNV: total neutralizing value; G: goodness-of-prediction criterium; MSE: Mean Squar Error.

3.5. Soil fertility management zones

Table 5 presents the results of the Kaiser–Meyer–Olkin (KMO) measure of sampling adequacy and Bartlett's test of sphericity. The Bartlett's test was highly significant ($p \leq 0.000$), indicating that the correlation matrix differs significantly from an identity matrix and that the soil

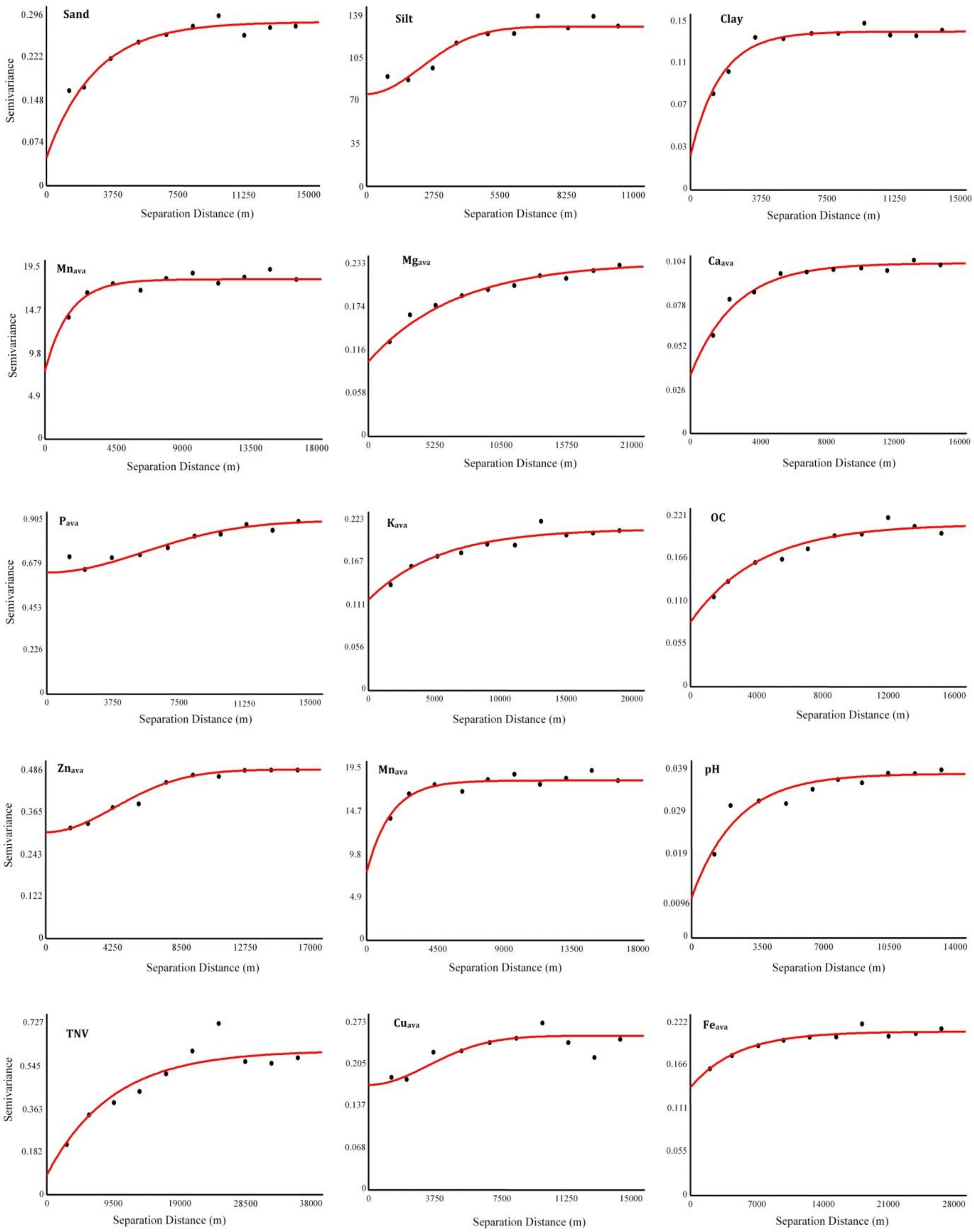

Figure 3. Semivariogram of soil properties in the study area, experimental semivariance (●) and the fitted semivarigram models (lines)

Table 5. Parameters of KMO and Bartlett's Test.

Kaiser-Meyer-Olkin Measure of Sampling Adequacy		0.669
Bartlett's Test of Sphericity	Approx. Chi-Square	1.215E3
	df	91
	Sig.	0.000

Table 6. Principal component analysis of soil properties and loading coefficient for the first four principal components.

PC	Eigen values	% of Variance	Cumulative (%)	SC
PC1	4.655	31.036	31.036	0.232
PC2	2.354	15.690	46.726	0.326
PC3	1.559	10.391	57.117	0.400
PC4	1.426	9.508	66.625	0.419
PC5	0.933	6.219	72.844	
PC6	0.824	5.494	78.338	
PC7	0.715	4.769	83.107	
PC8	0.643	4.289	87.396	
PC9	0.485	3.232	90.628	
PC10	0.381	2.538	93.167	
PC11	0.328	2.185	95.351	
PC12	0.284	1.891	97.242	
PC13	0.248	1.654	98.897	
PC14	0.165	1.103	100.000	
PC15	7.295E-16	4.863E-15	100.000	

PC: principal component, SC: selection criterion

variables are sufficiently interrelated for principal component analysis (PCA). The overall KMO value was 0.669, suggesting that the data are acceptable for factor analysis, as KMO values above 0.6 are generally considered to indicate an adequate level of common variance among variables. Therefore, the dataset was deemed suitable for subsequent PCA to derive composite variables for management zone delineation.

Principal components were extracted based on the correlation structure among soil variables, retaining only components with eigenvalues greater than 1. In total, four principal components (PCs) were selected for further analysis, together explaining 66.6% of the total variance in the dataset (Table 6, Figure 4). Principal Component 1 (PC1) accounted for 31.0% of the total variance and showed high loadings for nearly all soil properties, except for available Ca and pH, indicating that PC1 represents a general soil fertility gradient. Principal Component 2 (PC2) explained 15.7% of the variance and was mainly influenced by TNV, available P, Mg, Mn, Zn, pH, and clay content, suggesting that PC2 reflects a lime–nutrient–texture axis associated with soil reaction and fine-textured fractions.

Third principal component (PC3) explained 10.4% of the total variance and was dominated by available Ca, pH, and EC, indicating a component associated with soil reaction and salinity status. The fourth principal component (PC4) accounted for 9.5% of the variance and was mainly influenced by available K and P, representing a macronutrient fertility axis. Overall, these four PCs together captured the major gradients in soil fertility and related properties, consistent with previous studies in which three to four PCs summarized the variability of soil attributes in eastern India, northeast Iran, and tropical regions of southern India (Tripathi et al. 2015; Khaledian et al. 2017; Behera et al. 2018).

The PC1–PC2 biplot (Figure 5) revealed three major clusters of soil variables. The first group comprised available Mg, available K, silt, clay, and TNV, the second group included SOC and the available forms of Mn, Zn, P, Fe, and Cu, and the third group consisted of available Ca, EC, and sand. These groupings highlight the close association between SOC and micronutrient availability, as well as the linkage of EC and Ca with coarser textures.

The first four PCs were used as input variables for delineating soil fertility management zones. Fuzzy c-means clustering was performed using the FuzMe software to determine the optimal number of management zones. The fuzzy performance index (FPI) and normalized classification entropy (NCE) were used as clustering validity indices, and their joint minima indicated that four management zones (MZs) provided the most appropriate partitioning of the study area (Figure 6). Principal component loadings for each variable are presented in Table 7. Analysis of variance showed that the four delineated MZs differed significantly for most soil properties, confirming that the clustering successfully separated areas with distinct fertility characteristics, in agreement with earlier studies on MZ delineation (Shukla et al. 2017; Seyedmohammadi et al. 2018).

Also, the mean values of soil properties of four created MZs are presented in Table 8. Since the FPI and NCE had the minimum values at number four, so four MZs was selected. The illative map showing four MZs are presented in Figure 7.

4. Discussion

4.1. Characteristic and variability of soil properties

According to the standard framework proposed by Wilding et al. (1994), coefficients of variation (CV) between 0 and 15% indicate low variability, CV values of 15–35% indicate moderate variability, and CV values between 35 and 100% indicate high variability. In the

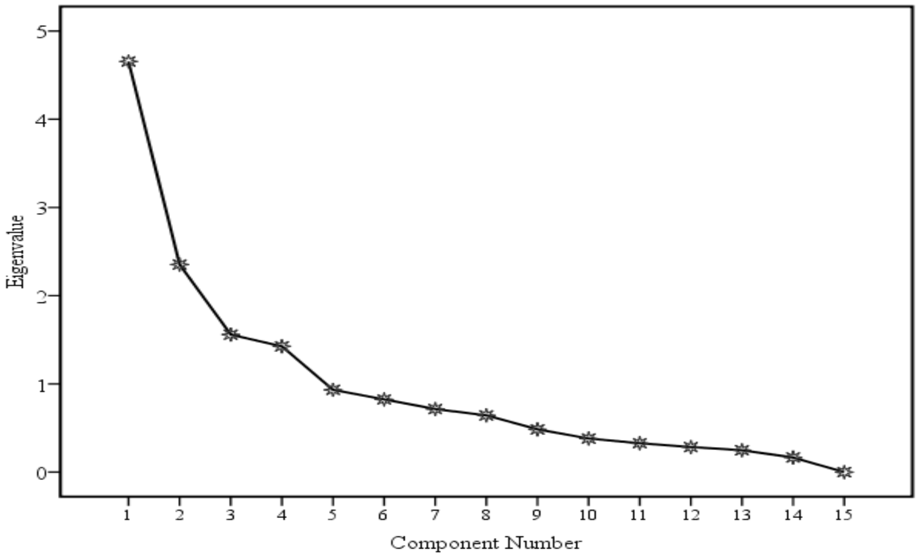

Figure 4. Scree plot describing Eigen values for each principal component

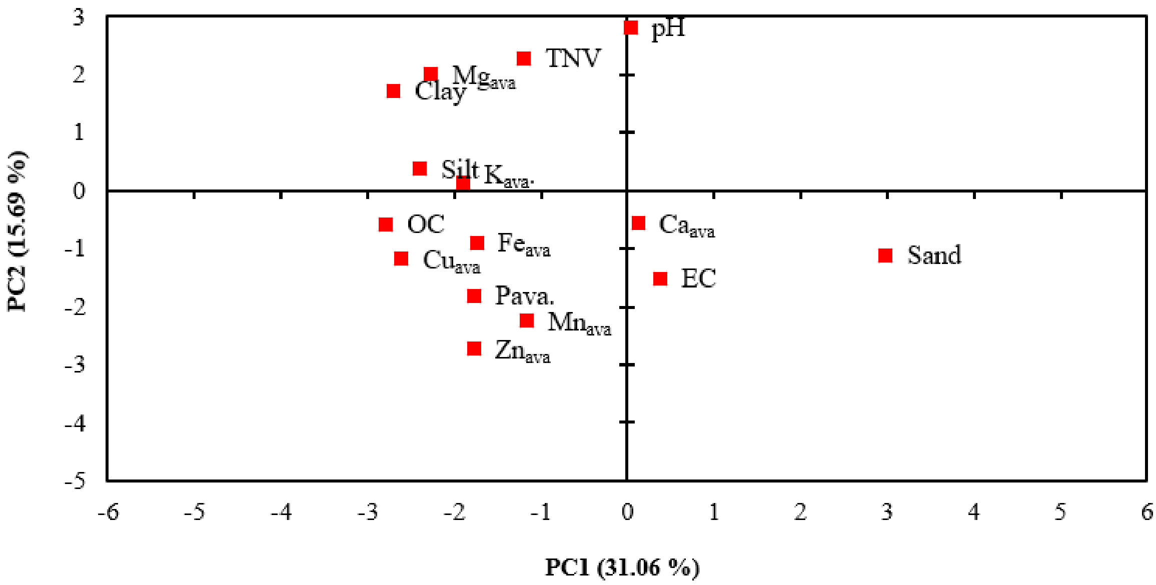

Figure 5. Principal component analysis bi-plot (PC1 vs PC2) of soil properties of the study area.

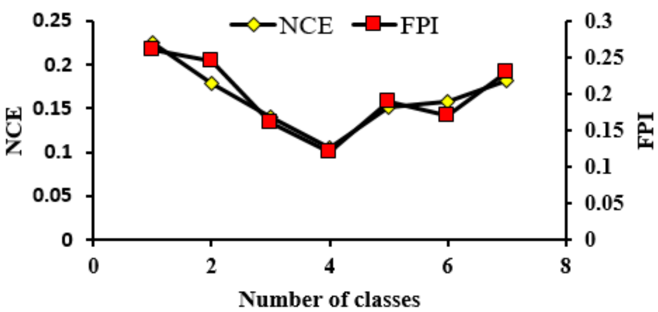

Figure 6. Fuzzy performance index (FPI) and normalized classification entropy (NCE) for different number of cluster classes.

Table 7. Principal component loading for each variable.

	OC	TNV	K	P	Ca	Mg	Fe	Mn	Zn	Cu	pH	EC	Sand	Silt	Clay
PC1	0.76	0.39	0.45	0.43	0.08	0.64	0.61	0.24	0.36	0.78	0.14	-0.22	-0.86	0.66	0.8
PC2	0.15	-0.56	-0.08	0.5	0.004	-0.48	0.26	0.49	0.75	0.26	-0.63	0.11	0.16	2.45×10^{-5}	-0.32
PC3	0.12	0.28	0.21	-0.007	0.56	0.19	-0.33	0.25	-0.09	-0.16	-0.48	0.75	-0.015	-0.09	0.15
PC4	0.21	0.31	0.42	0.57	-0.22	0.12	-0.02	-0.25	0.26	-0.12	0.26	0.07	0.39	-0.16	-0.027

Table 8. Variance analysis and comparison of mean criteria in four created for different management zones (MZs).

MZs	OC	TNV	K	P	Ca	Mg	Fe	Mn	Zn	Cu	pH	EC	Sand	Silt	Clay
	%					mg kg^{-1}					-	dS m^{-1}		%	
1	0.87^{a}	15.79^{a}	351.3^{ab}	11.36^{a}	2666.79^{a}	608.5^{a}	6.03^{a}	9.31^{a}	0.699^{a}	1.68^{a}	8.06^{a}	1.97^{a}	34.14^{ac}	36.88^{a}	28.97^{a}
2	1.13^{b}	15.12^{a}	392.7^{b}	22.85^{b}	3959.61^{b}	555.5^{a}	3.96^{b}	8.16^{a}	0.990^{b}	1.78^{ac}	7.78^{bc}	3.39^{b}	27.52^{a}	39.14^{a}	33.33^{b}
3	0.64^{c}	12.05^{b}	312.6^{a}	9.544^{a}	2921.16^{a}	432.1^{b}	3.82^{b}	12.73^{b}	0.870^{ab}	1.09^{b}	7.74^{b}	7.99^{c}	55.38^{b}	23.6^{b}	21.02^{c}
4	1.001^{bd}	9.73^{c}	315.76^{a}	25.02^{b}	2656.11^{a}	381.9^{b}	7.21^{c}	11.71^{b}	1.888^{c}	2.03^{c}	7.83^{c}	1.89^{a}	38.13^{c}	37.41^{a}	24.45^{c}

Hotelling's trace value is 4.569, F=17.679, $df_{Hypo.}=42$, $df_{Error}=488$, $P<0.0001$

Different letters within each column indicate significant difference between the management zones at $P<0.1$, comparison of mean criteria using LSD test.

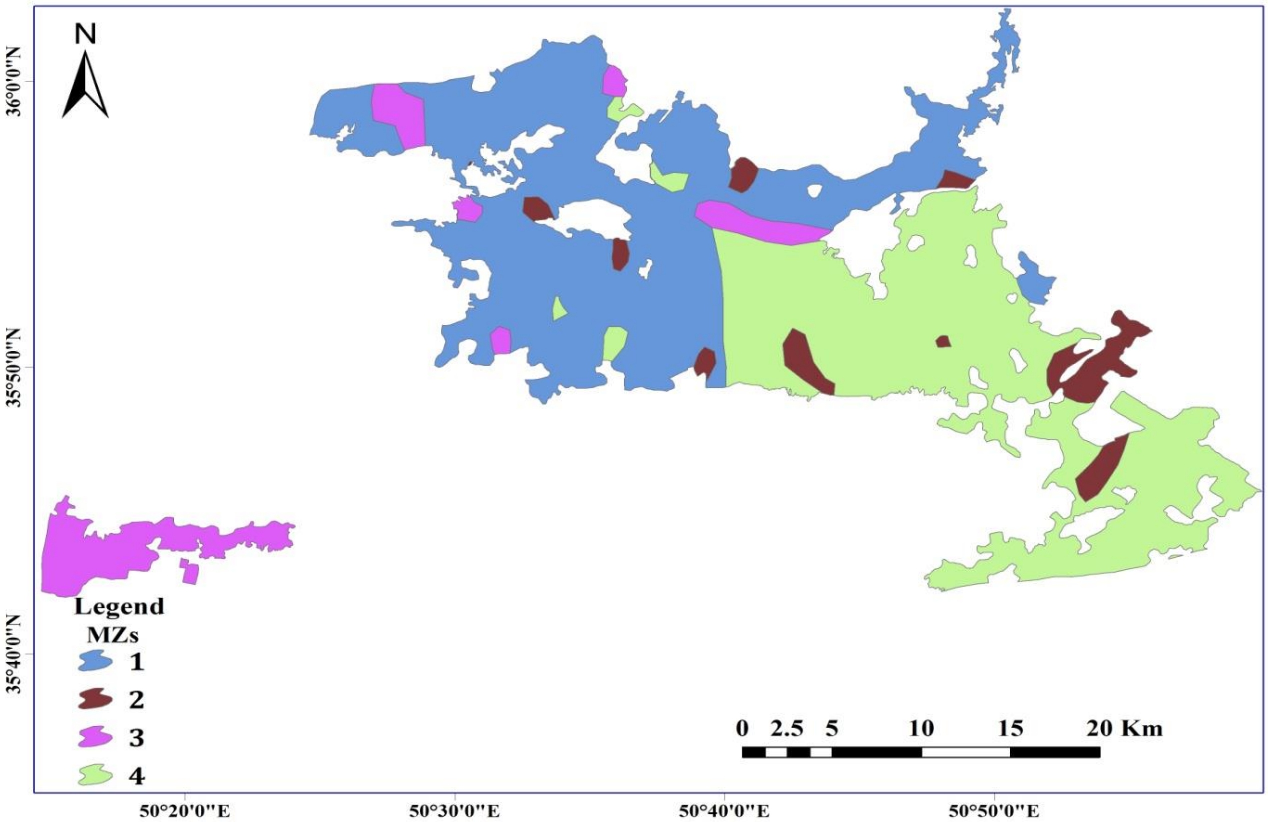

Figure 7. Soil management zones (MZs) of the study area.

present study, only pH exhibited low variability, whereas clay content and TNV fell into the moderate variability class, and all other soil properties—including available K, P, Mg, Fe, Mn, Zn, Cu, EC, sand, and silt—showed high variability. Soil pH had the lowest CV (2.68%), while available Fe had the highest CV (98.15%). These results are consistent with previous studies in northern Ethiopia and India, where pH showed the lowest CV among soil properties (Behera et al. 2018). Subhash et al. (2025), for example, reported CV values of 6.35, 47.09, 30.46, 59.31, and 37.27% for pH, EC, SOC, available P, and available K, respectively, and Guo et al. (2024) classified available P as having high variability, whereas pH, soil organic matter, and available K showed moderate variability in black soils. Wide variability in soil properties has also been documented in Egypt (Metwally et al., 2019), Ethiopia (Tiruneh et al., 2021), Kenya (Mwendwa et al., 2022), and India (Subhash et al., 2025). Several recent studies, including Zhang et al. (2022) and Subhash et al. (2025), have attributed high spatial variability in soil properties to the combined effects of soil-forming processes, topography, climatic conditions, soil–crop management practices, organic and inorganic fertilizer application, tillage operations, irrigation, and other anthropogenic activities. Overall, the CV values obtained in this study indicate a high degree of spatial variability for most soil properties, suggesting that delineation of management zones is both necessary and feasible under these conditions.

The results of this study are broadly consistent with recent investigations reporting relatively low spatial variability of soil pH but substantially greater variability in salinity-related and nutrient-related properties. Mwendwa et al. (2022) reported low CV values for soil pH (5.1–5.8%) but moderate variability in available P (36.2%) in agricultural soils of Kenya. Similarly, Subhash et al. (2025) found that pH had the lowest variability (CV = 6.35%), whereas EC (47.09%), available P (59.31%), and available K (37.27%) exhibited high spatial variability in Vertisols of central India. Vimalashree et al. (2024) also observed the greatest variability for available K_2O (CV = 60.57%), while pH showed comparatively low variation. Therefore, the low CV of pH (2.68%) and the high CVs of EC and plant-available nutrients in the present study follow the general pattern reported in recent literature. The particularly high variation in available Fe (98.15%) may be associated with local differences in carbonate content, texture, moisture regime, redox conditions, organic matter distribution, and fertilizer or irrigation history. Collectively, these findings confirm considerable within-area heterogeneity and support the use of management-zone delineation and site-specific nutrient and salinity-management practices.

4.2. Spatial variability analysis

Nugget values, which represent microscale variability and measurement error, were generally low for most soil properties (ranging from 0.009 to 0.566), except for available Mn (8.0) and silt (75.1). The relatively large nugget values for silt and available Mn indicate that these variables are more strongly influenced by short-range ecological processes or that the chosen sampling interval was not sufficiently fine to capture their spatial dependence. In other words, the sampling distance may have been too coarse to adequately describe the spatial structure of these properties (Behera et al. 2018). Sill values were also relatively high for silt (130) and available Mn (19.5), whereas for the other soil properties they ranged from 0.037 (pH) to 2.84 (EC). Recent geostatistical studies have likewise documented substantial differences in nugget and sill parameters among soil attributes. For example, Vimalashree and Sathish (2024) reported that nugget and sill values, together with their ratio, varied markedly among pH, organic carbon, available N, P, K, S, and Zn, reflecting property-specific differences in short-distance variation and spatial continuity. In the present study, the comparatively large nugget values of silt (75.1) and available Mn (8.0), together with their moderate DSD values of 0.578 and 0.432, respectively, indicate that a considerable proportion of their total variability occurred at distances shorter than the sampling interval or was associated with unresolved local variation and/or analytical uncertainty. This interpretation is consistent with the geostatistical meaning of the nugget effect, which may represent measurement error, microscale heterogeneity, or both. In contrast, the low nugget-to-sill ratios of TNV (0.125), EC (0.146), clay (0.211), pH (0.241), and sand (0.246) suggest that their spatial variation was more consistently captured at the sampling scale used in this study.

Based on the degree of spatial dependence (DSD) values (Table 3), pH, EC, sand, TNV, and clay exhibited strong spatial dependence (DSD < 0.25), indicating that their spatial patterns are governed mainly by intrinsic soil factors such as parent material, mineralogy, and texture. The remaining soil properties showed moderate spatial dependence. The present findings are comparable with recent studies showing that the degree of spatial dependence differs substantially among soil properties, even within the same agricultural landscape. Yeneneh et al. (2022) reported strong spatial dependence for soil pH, EC, exchangeable acidity, exchangeable K, and CEC, based on nugget-to-sill ratios below 25%. Similarly, the strong spatial dependence observed here for pH, EC, sand, TNV, and clay indicates that these properties were predominantly structured by relatively stable spatial controls. However, the moderate dependence of SOC, available K, P, Ca, Mg, Fe, Mn, Zn, and Cu suggests a combined influence of inherent soil-forming factors and spatially heterogeneous management practices. This pattern is also consistent with a recent study in the Tigris Basin, where the degree of spatial dependence differed among micronutrients, with Fe and Cu exhibiting lower

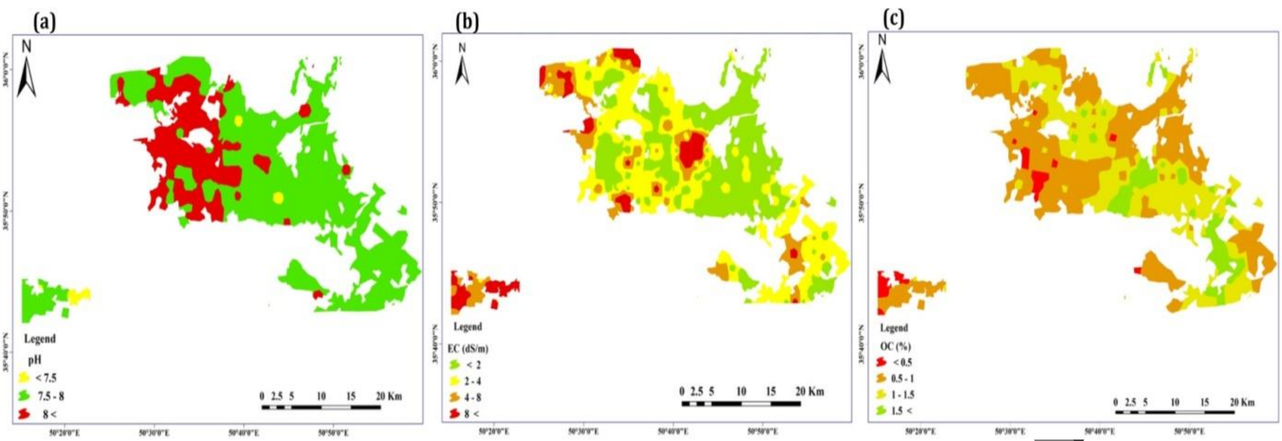

Figure 8. Distribution maps of pH (a), EC (b), OC (c) of the study area by Ordinary kriging method.

dependence than Zn and Mn. In contrast, Wani et al. (2016) reported weak spatial dependence for available P and K and moderate dependence for EC in their study. A wide range of spatial dependence classes has been observed, reflecting the combined influence of intrinsic factors (e.g. soil-forming processes, parent material, climate) and extrinsic factors (e.g. cultivation practices, fertilizer use, irrigation) on the spatial patterns of soil properties. It should also be noted that the spatial dependence classification proposed by Cambardella et al. (1994) has inherent limitations, as it does not explicitly account for the range parameter. In this study, the DSD values ranged from 0.125 to 0.7, corresponding to strong to moderate spatial dependence. TNV, EC, pH, clay, and sand had broadly similar DSD ratios, but the effective range for clay was shorter than for the other variables, indicating that clay reached its maximum variance over shorter lag distances and thus exhibited stronger short-range spatial variation. In contrast, TNV had the lowest DSD ratio while showing a larger range than clay, a pattern also observed for EC, which combined a relatively low DSD with a comparatively large range.

Semivariogram analysis (Figure 2) showed that the ranges of spatial dependence for the studied soil properties varied from 1,650 m (available Mn) to 105,600 m (EC) (Table 3). The large ranges for EC, TNV, available P, and available Mg suggest that these properties are influenced by factors operating over broader spatial scales, such as regional climatic gradients, irrigation schemes, or fertilizer application patterns, compared with properties like available Mn, clay, and pH, which showed shorter effective ranges and more localized variability.

The wide contrast in effective ranges observed in the present study further emphasizes that the controlling processes operated at different spatial scales. EC showed the largest range (105,600 m), followed by TNV (9,400 m), available P (7,800 m), available Mg (7,010 m), and available Zn (6,280 m), indicating that their values remained spatially autocorrelated over relatively broad distances. In comparison, available Mn (1,650 m), clay (1,700 m), pH (2,400 m), and exchangeable Ca (2,700 m) exhibited shorter ranges, suggesting more localized spatial structures. Recent studies have also demonstrated considerable differences in variogram models and spatial-dependence patterns among pH, EC, organic carbon, available P, available K, and soil-texture fractions. For example, Subhash et al. (2025) found that exponential models best described pH, EC, SOC, available P, and sand, whereas Gaussian, spherical, circular, and other models were more appropriate for other soil properties, confirming that no single spatial model or scale can adequately represent all soil variables within an agricultural landscape. Therefore, the large range of EC in the present study may reflect broad-scale controls, whereas the short range of available Mn and clay indicates a need for denser sampling if their local spatial patterns are to be mapped more precisely.

4.3. Spatial interpolations of soil properties

The interpolated maps revealed distinct spatial distribution patterns for the different soil properties across the study area. Approximately 1.3, 72.9, and 25.8% of the area had soil pH values of <7.5, 7.5–8.5, and >8.5, respectively (Figure 8a), indicating that slightly to moderately alkaline conditions dominate most of the irrigated wheat fields. A large portion of the study area was non-saline, with 77.82% of the land having EC values <4 dS m^{-1} and 22.18% having EC values >4 dS m^{-1} (Figure 8b), suggesting that salinity is a concern in about one-fifth of the region. Soil OC displayed a mosaic pattern, with 55.4% of the area having SOC <1% (Figure 8c), 34.72% between 1 and 1.5%, and 9.84% >1.5%. A similar patchy distribution of SOC has been reported by Behera et al. (2018), who attributed such patterns to interactions among land-use and management practices, microclimatic differences, and biotic processes controlling organic matter inputs and decomposition. In the present study, the observed mosaic distribution of SOC likely reflects spatially variable crop residue management, manure application, and irrigation practices, emphasizing the need for site-specific strategies to improve organic carbon levels and, consequently, soil fertility and structure.

The spatial patterns of pH, EC, and SOC observed in the present study are consistent with recent geostatistical investigations showing that these properties can display contrasting spatial structures within cultivated landscapes. Khan et al. (2021), using GIS-based kriging in diversified cropping regions of Bangladesh, found that pH, EC, SOC, and available nutrients differed markedly in their spatial distribution and degree of dependence, supporting the use of soil-property maps for site-specific nutrient management. Similarly, Subhash et al. (2025) reported relatively low variability in pH but greater heterogeneity in EC and SOC in soybean–wheat Vertisols of central India. In the present study, the predominance of alkaline soils, the occurrence of salinity in 22.18% of the area, and the mosaic distribution of SOC, with 55.4% of the area containing less than 1% SOC, indicate that carbon management and salinity management should be integrated rather than addressed uniformly across all fields.

+1

Production of plant biomass, litter deposition, and subsequent decomposition are the key processes controlling SOC dynamics (Behera et al. 2018). The low SOC content observed in the studied agricultural lands undoubtedly limits the productive capacity of these soils and constrains the achievement of sustainable wheat yields. Field studies in Iran have shown that each 1 g kg^{-1} increase in SOC (equivalent to 0.1% or about 3 t ha^{-1} of organic matter) can increase wheat grain yield by approximately 286 kg ha^{-1}, particularly in soils with low clay content and elevated salinity. Organic amendments such as composted poultry manure can enhance soil fertility by supplying organic matter and nutrients, but their efficacy depends on the compost's chemical and biological properties. Moreover, increasing SOC can partially offset the negative effects of salinity (EC up to about 10.5 $dS.m^{-1}$) and light texture (clay <15%) on wheat grain yield (Comprehensive Soil Fertility and Plant Nutrition Program, 2015). Ghaley et al. (2018) and other studies have similarly reported that enhancing SOC has pronounced positive effects on winter wheat grain yield and aboveground biomass. These findings underline the importance of assessing SOC status in agricultural lands to support improved management decisions by farmers, extension advisors, and policy makers aiming at both yield improvement and long-term soil health.

4.4. Spatial patterns of available Fe and implications

According to the kriged maps, lower concentrations of available Fe were observed in the western part of the study area (Figure 9a). About 1.2% and 10.98% of the area had Fe_{ava} values <3.5 mg kg^{-1} and 3.5–4.5 mg kg^{-1}, respectively. Based on the Comprehensive Soil Fertility and Plant Nutrition Program (2015), Fe_{ava} concentrations <5 mg kg^{-1} are classified as low and indicate a high probability of Fe deficiency. Under such conditions, the application of Fe fertilizers can increase relative wheat grain yield by approximately 50–75%, particularly in calcareous and saline–alkaline soils where Fe availability is strongly constrained. These results suggest that targeted Fe fertilization in Fe-deficient management zones could substantially narrow existing yield gaps while avoiding blanket micronutrient applications across the entire region.

A large portion of the study area had Fe_{ava} concentrations between 4.5 and 8.5 mg kg^{-1}, which falls within the medium range for available Fe, where the application of Fe fertilizers can increase relative wheat yield by approximately 75–100%. In addition, about 7.52% of the study area had Fe_{ava} concentrations greater than 8.5 mg kg^{-1}, corresponding to high Fe availability (>7.5 mg kg^{-1}), where further Fe fertilization is unlikely to produce any appreciable yield response.

The spatial variability map of available Zn (Figure 9b) showed a pattern similar to that of Fe_{ava}, with the western region of the study area exhibiting the lowest Zn_{ava} concentrations. Approximately 27%, 33%, and 40% of the area had Zn_{ava} values <0.7, 0.7–1.2, and >1.2 mg kg^{-1}, respectively. Consequently, more than 55% of the study area had Zn_{ava} concentrations below 1 mg kg^{-1}, indicating a high probability of yield response to Zn fertilization in these zones, whereas in areas with Zn_{ava} >1 mg kg^{-1}, additional Zn application is unlikely to increase wheat yield.

The spatial distribution of available Mn (Figure 9c) showed that only about 8% of the study area had Mn_{ava} concentrations <6 mg kg^{-1}, which can be classified as low Mn. Thus, Mn deficiency appears to be restricted to a relatively small fraction of the irrigated lands in Alborz province. Approximately 21% and 71% of the area had medium and high Mn_{ava} concentrations, respectively, suggesting that Mn fertilization is generally unnecessary except in localized deficiency hotspots.

Examination of the distribution maps for Fe_{ava}, Zn_{ava}, Mn_{ava}, and pH indicates that the spatial variability of these micronutrients is strongly controlled by pH gradients. As noted by Havlin (2015), the availability of Fe, Zn, and Mn decreases with increasing soil pH, particularly in calcareous, alkaline soils. In the western part of Alborz province, where soil pH values are higher than in other regions, the concentrations of available Fe, Zn, and, to a lesser extent, Mn were correspondingly lower, underscoring the need for pH-sensitive micronutrient management in these areas.

The spatial differentiation of DTPA-extractable Fe, Zn, and Mn observed in this study is comparable with the findings of Gökmen et al. (2023), who reported pronounced spatial variability in soil micronutrients across

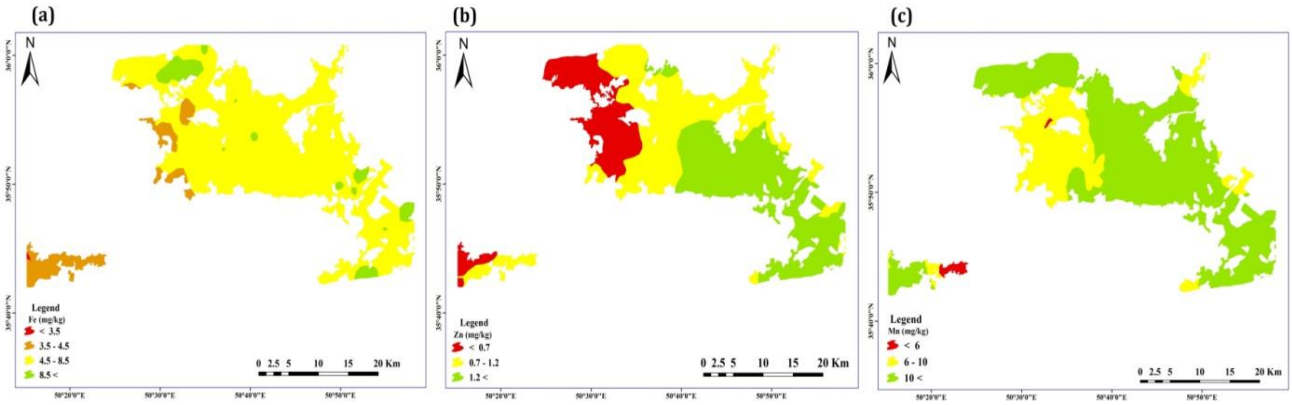

Figure 9. Distribution maps of Fe_{ava} (a), Zn_{ava} (b), Mn_{ava} (c) of the study area by Ordinary kriging.

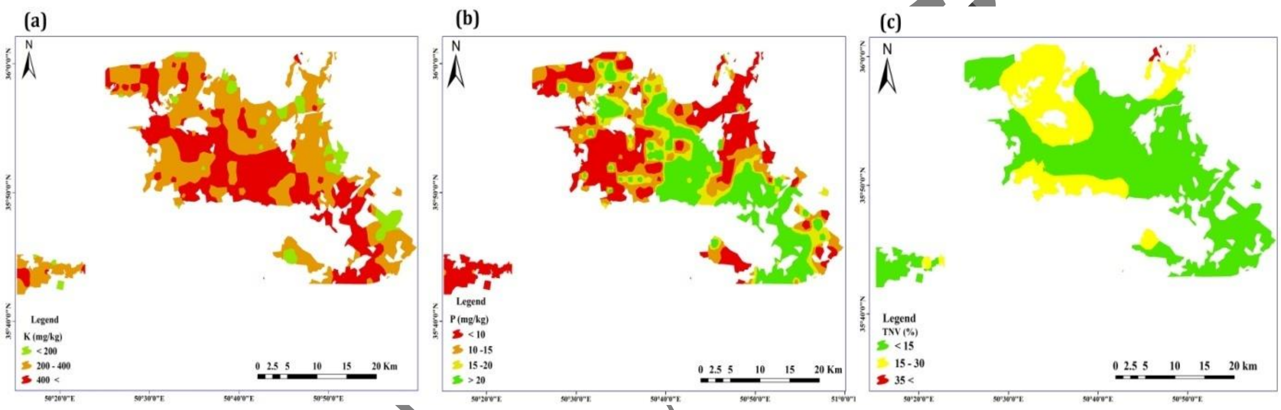

Figure 10. Distribution maps of K_{ava} (a), P_{ava} (b), TNV (c) of the study area by Ordinary kriging

the Upper Tigris Basin and showed that the degree of spatial dependence differed among Fe, Cu, Zn, and Mn. In the present study, Fe and Zn deficiencies were concentrated mainly in the western part of the study area, where pH was relatively higher, whereas low Mn was confined to a smaller proportion of the irrigated wheat lands. This contrast suggests that Fe and Zn may be more sensitive than Mn to the combined effects of alkalinity, carbonate-related reactions, and localized soil-management conditions in the study area. Nevertheless, because micronutrient availability is also influenced by SOC, TNV, moisture regime, and redox conditions, the observed spatial correspondence should be regarded as an association rather than direct evidence of pH control. Tarar et al. (2020) used ordinary kriging to map DTPA-extractable Zn, Cu, Fe, and Mn in Punjab, Pakistan, and reported significant negative relationships between soil pH and the plant-available concentrations of Zn, Fe, and Mn. Likewise, Dhaliwal et al. (2022) demonstrated that the distribution of DTPA-extractable Zn, Fe, Mn, Cu, and Ni was influenced by parent material, land-use system, and soil depth. The lower Fe and Zn concentrations in the relatively more alkaline western part of the present study area are therefore consistent with the reduced availability of these micronutrients at high pH; however, the spatial pattern may also reflect concurrent variation in TNV, SOC, texture, moisture conditions, and management history.

Ordinary-kriged maps of available K, available P, and TNV are shown in Figures 10a, 10b, and 10c, respectively. According to Figure 10a, about 88% of the study area had K_{ava} concentrations >200 mg kg^{-1}, indicating that most irrigated wheat fields in Alborz province have high K status and, under current conditions, blanket application of K fertilizers is not warranted. This highlights the potential for cost savings and reduced environmental impact through site-specific K management based on the delineated fertility management zones.

The spatial distribution of available P (P_{ava}) is shown in Figure 10b. Approximately 36.2%, 20.6%, and 43.0% of the study area had low (<10 mg kg^{-1}), moderate (10–15 mg kg^{-1}), and high (>15 mg kg^{-1}) P_{ava} values, respectively. Accordingly, P fertilization is recommended for the low and moderate P zones, where a yield response is likely, whereas areas with high P_{ava} are unlikely to benefit from additional P inputs and should be managed without blanket P application.

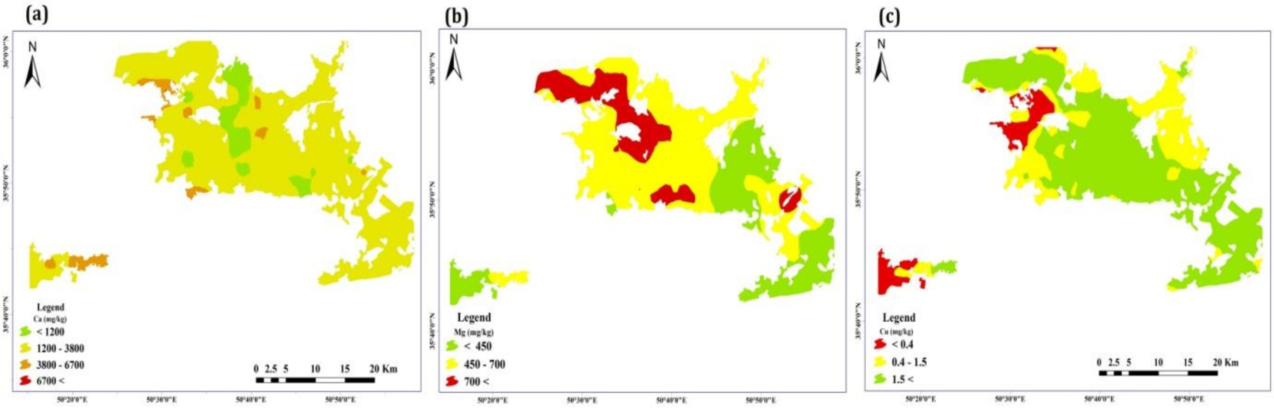

Figure 11. Distribution maps of Ca_{ava} (a), Mg_{ava} (b) and Cu_{ava} (c) of the study area by Ordinary kriging.

The contrasting spatial distributions of available P and K in the present study are in line with recent nutrient-mapping studies, which have shown that macronutrient status may vary considerably within agricultural landscapes. Nalin et al. (2023) demonstrated that the spatial variation of plant-available P in a southern Brazilian farm was partly explained by environmental covariates, indicating that the distribution of available P is influenced by both soil-forming factors and field-scale conditions. In addition, Guo et al. (2024) reported substantial spatial and temporal variation in available P and K, highlighting that nutrient-management recommendations should be based on the mapped status of individual nutrients rather than on uniform field-level applications. Therefore, the predominance of K-sufficient areas in the present study, together with the occurrence of low- and moderate-P zones over 56.8% of the area, supports withholding routine K fertilization in high-K zones while prioritizing P inputs in areas with an identified probability of P response.

4.5. Spatial variability of TNV

The spatial distribution of total neutralizing value (TNV) is presented in Figure 10c. About 71% of the study area had TNV values <15%, indicating predominantly low to moderate carbonate content. In contrast, 28.8% of the area had TNV between 15 and 35%, and a small fraction (0.27%) had TNV >35%, reflecting highly calcareous conditions. These patterns highlight the potential for localized pH and carbonate-related constraints on nutrient availability, particularly in the more calcareous zones.

4.6. Spatial variability of Ca_{ava}, Mg_{ava}, and Cu_{ava}

The spatial variability maps of available Ca, Mg, and Cu (Figures 11a, 11b, and 11c) show that most of the study area has Ca_{ava} concentrations below 3,800 mg kg^{-1}. For Mg_{ava}, approximately 33%, 48%, and 19% of the area had values <450, 450–700, and >700 mg kg^{-1}, respectively, indicating that only limited zones may require Mg fertilization. The interpolated Cu_{ava} map shows that about 10% of the area had Cu_{ava} <0.4 mg kg^{-1}, whereas a large portion (around 70%) had adequate Cu levels and would not require Cu fertilization. These results emphasize the importance of site-specific micronutrient management to avoid unnecessary inputs in nutrient-sufficient areas while targeting deficiencies in specific zones.

The spatial distribution of soil texture parameters is shown in Figure 12. The ordinary-kriged map of sand (Figure 12a) indicates that only three relatively small regions in the western part of the study area are light-textured. The observed deficiencies of available Cu, Zn, Fe, and, to some extent, Mn in these areas can be attributed to the combination of light texture and low SOC, which together enhance nutrient leaching and reduce micronutrient retention in the rooting zone.

According to Figure 12b, about 65% and 32% of the study area have silt contents of 20–40% and >40%, respectively, while only 3% has silt <20%. The spatial distribution of clay content (Figure 12c) shows that heavy-textured soils (clay >40%) are not widespread in the irrigated wheat lands of Alborz province; these heavier soils occur mainly in the northern part of the study area. This pattern suggests that most fields have medium-textured soils, where targeted improvements in SOC and careful management of irrigation and fertilization can substantially enhance nutrient use efficiency, whereas the limited light-textured zones require particular attention to SOC buildup and micronutrient management to mitigate leaching losses.

The joint interpretation of texture, SOC, and micronutrient maps is also supported by recent spatial-variability research. Velamala et al. (2024) evaluated pH, EC, OC, available macronutrients, and DTPA-extractable micronutrients using ordinary kriging and found substantial spatial variation in EC, Zn, and Cu, as well as widespread nutrient deficiencies in particular zones. Gökmen et al. (2023) similarly demonstrated that the spatial dependence and distribution patterns of Fe, Cu, Zn,

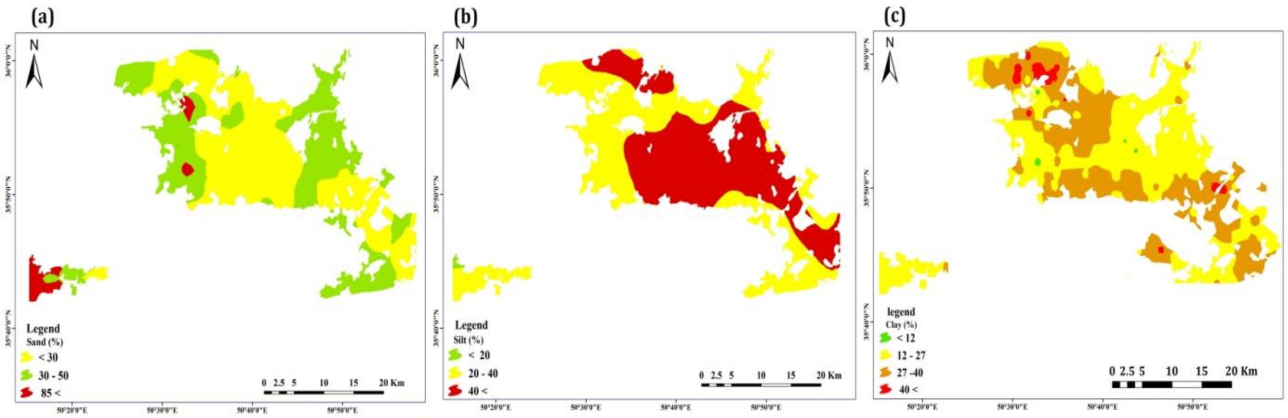

Figure 12. Distribution maps of sand (a), silt (b) and clay (c) of the study area by Ordinary kriging.

and Mn differed across the Upper Tigris Basin, indicating that micronutrient-management zones should be delineated separately rather than inferred from a single soil indicator. In the present study, the co-occurrence of light-textured soils and low SOC in limited western areas may reduce nutrient-retention capacity and may contribute to the lower concentrations of Fe, Zn, Cu, and Mn observed in these zones. Hence, integrating texture, SOC, TNV, pH, EC, and micronutrient maps would provide a more reliable basis for targeted fertilization, organic-amendment application, and irrigation management.

4.7. Soil fertility management zones

The geographical extents of MZ1, MZ2, MZ3, and MZ4 were 35%, 13%, 20%, and 32% of the study area, respectively. The highest SOC content was observed in MZ2, and SOC followed the order MZ2 > MZ4 > MZ1 > MZ3, with significant differences among zones ($p < 0.1$). These results indicate that particular efforts are needed to increase SOC in MZ1 and MZ3, which have the lowest SOC levels and therefore the greatest potential benefit from organic matter additions and residue management.

Soil texture in MZ1 and MZ2 is generally heavier than in MZ3 and MZ4. Under such conditions, the application and conservation of organic amendments are essential to maintain favorable soil structure, improve infiltration, and enhance root growth. Composted poultry manure is an organic amendment that can be used to improve the quality and nutritional value of organic materials in agricultural systems.

The mean pH in the four delineated zones ranged from 7.74 to 8.06 and differed significantly among MZs ($p < 0.1$). The highest pH values were recorded in MZ1 and the lowest in MZ3, reflecting differences in TNV and parent material across the zones.

The highest mean EC (7.99 dS m^{-1}) was recorded in MZ3, exceeding the commonly accepted threshold of 6 dS m^{-1} for wheat, indicating that salinity is a serious constraint in this zone and requires careful management of irrigation water quality, fertilizer inputs, and cultivar choice. In such areas, yield reductions are likely due to salinity stress. Although the mean EC in MZ2 was below the critical threshold for wheat, salinity levels should be monitored and managed to prevent yield losses. The lowest EC values occurred in MZ4, and EC did not differ significantly between MZ1 and MZ4, suggesting that salinity is less of a concern in these zones.

Overall, soil properties differed significantly among the four MZs. The observed heterogeneity can be attributed to differences in soil type, parent material, and management practices, including fertilization and irrigation. The delineation of MZs thus provides a practical framework for farmers and policymakers to adopt site-specific soil and nutrient management strategies aimed at sustainable soil conservation, reduced degradation, and increased wheat production. In practice, farmers can use the mean values of soil properties within each MZ as reference levels for designing variable-rate fertilizer recommendations Nawar et al. 2017; Behera et al. 2018).

For example, the mean K_{ava} values in all four MZs exceeded 200 mg kg^{-1}, which is commonly considered the critical level for wheat. Under these conditions, K fertilization is not required for wheat production, and yield responses to K are unlikely, especially where K_{ava} exceeds 250 mg kg^{-1}. In contrast, the critical level of P_{ava} for wheat is about 15 mg kg^{-1}. The mean P_{ava} values in MZ1 and MZ3 were below this threshold, indicating that additional P inputs would be needed to improve wheat productivity in these zones, whereas mean P_{ava} in MZ2 and MZ4 exceeded 15 mg kg^{-1}, suggesting limited likelihood of response to further P fertilization.

The mean Fe_{ava} concentration exceeded its critical value (approximately 4.5 mg kg^{-1}) in MZ1 and MZ4, but was lower in MZ2 and MZ3, indicating that Fe fertilization is most relevant in the latter two zones. Although the average Zn_{ava} values in MZ1 and MZ3 are close to the critical limit (0.7 mg kg^{-1}) and those in MZ2 and MZ4 are slightly higher, Zn fertilization may still increase yields in parts of all four zones, particularly in fields with Zn_{ava} values below 1 mg kg^{-1}. In summary, the distinct soil fertility profiles of the four MZs call for differentiated management options tailored to the specific constraints and nutrient status of each zone.

The practical utility of MZs ultimately depends on their simplicity, effectiveness, and economic feasibility from the perspective of farmers and crop production managers. Cluster analysis and fuzzy c-means clustering provide a robust basis for identifying and delineating such zones in irrigated wheat systems and for supporting the adoption of site-specific management strategies. The same approach can readily be extended to other cropping systems to improve nutrient use efficiency and reduce unnecessary fertilizer applications. In essence, cluster-based delineation of MZs contributes in two key ways: (i) by reducing within-zone variability, it facilitates site-specific soil management and more accurate variable-rate fertilization; and (ii) by summarizing spatial variability into a limited number of zones, it reduces the number of soil samples required for monitoring and thereby supports more efficient design of future soil sampling and management programs.

The delineation of four distinct Management Zones (MZs) captures the complex interplay between pedogenic background and agronomic management. The differentiation of these zones was largely driven by a general fertility gradient (PC1) and a lime-nutrient-texture axis (PC2). The emergence of these distinct spatial patterns confirms that soil properties in the Alborz province do not vary randomly but self-organize along gradients of water movement, topographic micro-variations, and historical fertilizer application. This multivariate clustering provides a scientific basis for transitioning from uniform field management to site-specific interventions. By understanding the underlying processes—such as carbonate-induced micronutrient fixation in MZ2 or salt accumulation in MZ4—farmers can implement targeted amelioration strategies, such as variable-rate gypsum application or spatially optimized organic amendments, rather than simply adjusting NPK rates (Libohova et al., 2025; Wang et al., 2026).

"From an agronomic perspective, delineating these MZs offers a practical roadmap for sustainable wheat production in the Alborz province. For instance, high-salinity zones require specific interventions such as leaching practices, applying gypsum, or selecting salt-tolerant wheat cultivars, rather than increasing fertilizer rates which could exacerbate osmotic stress. Meanwhile, in zones characterized by low SOC and micronutrient deficiencies, farmers should prioritize organic amendments and foliar application of Zn and Fe. Adopting such Variable Rate Technology (VRT) strategies based on these delineated MZs will not only optimize wheat yield and fertilizer use efficiency but also mitigate the environmental risks associated with agrochemical leaching."

5. Conclusions

In precision agriculture and site-specific crop management, agricultural inputs must be matched to the local requirements of soils and plants rather than applied uniformly across fields. In this study, the spatial distributions of key soil properties in irrigated wheat fields of Alborz province, Iran, were characterized using geostatistical methods, and the fields were subsequently partitioned into four soil fertility management zones using principal component analysis and fuzzy c-means clustering. The studied soil properties exhibited wide variation, with most variables showing moderate to high coefficients of variation and clear spatial heterogeneity. Geostatistical analysis indicated that exponential and Gaussian semivariogram models best described the spatial structure of the soil properties, and most variables displayed moderate to strong spatial dependence.

The four delineated MZs differed significantly in terms of SOC, salinity, pH, texture, and macro- and micronutrient status, reflecting both intrinsic soil factors and management-induced variability. Within each zone, the mean values of soil properties can be used as reference levels for developing variable-rate fertilizer prescriptions and other site-specific interventions. The resulting MZ maps provide a valuable decision-support tool for farmers, extension agents, and soil specialists to optimize fertilizer application, improve nutrient use efficiency, and design more efficient soil sampling schemes for irrigated wheat and other crops in the region. Ultimately, the adoption of such zone-based, site-specific management has the potential to increase wheat yields, reduce input costs, and contribute to long-term soil and environmental sustainability.

Acknowledgements

The authors gratefully acknowledge the support of the Soil and Water Research Institute (SWRI) and express their sincere thanks to all members of its Soil and Water Laboratory for their assistance with field sampling and laboratory analyses. The authors also thank the editor and anonymous reviewers for their constructive comments and suggestions, which helped to improve the quality of this manuscript.

References

Aggelopooulou K, Castrignan A, Gemtos T, et al. (2013) Delineation of management zones in an apple orchard in Greece using multivariate approach. Computers and Electronics in Agriculture 90:119-130. DOI: 10.1016/j.compag.2012.09.009

Agterberg FP (1984) Trend surface analysis. In: Gaile GL, Willmott CJ, (Eds.), Spatial Statistics and Models. Reidel, Dordrecht, the Netherlands, pp174-171. . DOI: 10.1007/978-94-017-3048-8_8

Alborz Meteorology Office (2026) Karaj, Alborz

province, Iran.
Barrena-González, J., Gabourel-Landaverde, V.A., Mora, J., et al. (2023). Exploring soil property spatial patterns in a small grazed catchment using machine learning. Earth Science Informatics, 16, 3811-3838. DOI: 10.1007/s12145-023-01125-1
Behera SK, Ravi K, Mathura RK, et al. (2018) Spatial variability of soil properties and delineation of soil management zones of oil palm plantations grown in a hot and humid tropical region of southern India. Catena, 165:251-259.
DOI: 10.1016/j.catena.2018.02.008
Behera SK, Suresh K, Rao BN, et al. (2016) Spatial variability of some soil properties varies in oil palm (Elaeis guineensis Jacq.) plantations of west coastal area of India. Solid Earth 7:979-993. DOI: 10.5194/se-7-979-2016, 2016.
Bevington J, Piragnolo D, Teatini P, et al. (2016) On the spatial variability of soil hydraulic properties in a Holocene coastal farmland. Geoderma 262:294-305. DOI: 10.1016/j.geoderma.2015.08.025
Burgess TM, Webster R (1980) optimal interpolation and isarithmic mapping of soil properties. II. Block kriging. Journal of Soil Science 31:333-341. DOI: 10.1111/j.1365-2389.1980.tb02085.x
Cambardella CA, Moorman TB, Novak JM, et al. (1994) Field scale variability of soil properties in central Iowa soils. Soil Science Society of America Journal 58:1501-1511.
DOI: 10.2136/sssaj1994.03615995005800050033x
Comprehensive soil fertility and plant nutrition program (2015) Guidelines for integrated soil fertility and plant nutrition management in strategic crops production. Soil and water research institute, Agricultural Research, Education and Extension Organization (AREEO), ministry of Jihad-e-agriculture, Tehran, Iran.
Davatgar N, Neishabouri MR, Sepaskhah AR (2012) Delineation of site specific nutrient management zones for a paddy cultivated area based on soil fertility using fuzzy clustering. Geoderma 173-174:111-118. DOI: 10.1016/ j.geoderma .2011 .12.005
Denton OA, Aduramigba-Modupe VO, Ojo AO, et al. (2017) Assessment of spatial variability and mapping of soil properties for sustainable agricultural production using geographic information system techniques (GIS). Cogent Food & Agriculture 3:1279366. DOI: 10.1080/23311932.2017.1279366
Dhaliwal, S. S., Naresh, R. K., Mandal, A., Walia, M. K., Gupta, R. K., Singh, R., & Dhaliwal, M. K. (2022). The pedospheric variation of DTPA-extractable Zn, Fe, Mn, Cu, and Ni in soils of India: A review. Sustainability, 14(1), 29.
https://doi.org/10.3390/su14010029.
Doetterl, S., Berhe, A. A., Heckman, K., et al. (2025). A landscape-scale view of soil organic matter dynamics. Nature Reviews Earth & Environment, 6, 67-81. DOI: 10.1038/s43017-024-00621-2
Gamma design, Inc. (2026) GS^{+} User's Manual for Windows. Gamma design software, plainwell, Michigan, USA.
Gee GW, Buder JW (1986) Particle size analysis. In: Klute, A., et al. (Ed.), Methods of Soil Analysis. Part 1. Agron. Monogr. 9. ASA and SSSA, Madison, WI, pp. 404-407. DOI: 10.2136/sssabookser5.1.2ed.c15
Ghaley BB, Wösten H, Olesen JE, et al. (2018) Simulation of soil organic carbon effects on long-term winter Wheat (Triticum aestivum) production under varying fertilizer inputs. Frontiers in Plant Science 9, article No. 1158. DOI: 10.3389/fpls.2018.01158
Gökmen, V., Sürücü, A., Budak, M., & Bilgili, A. V. (2023). Modeling and mapping the spatial variability of soil micronutrients in the Tigris basin. Journal of King Saud University—Science, 35 (6), 102724. https://doi.org/10.1016/j.jksus.2023.102724
Guo, B. X., et al. (2024). Spatial and temporal variability of soil pH, organic matter, available hydrolysable nitrogen, phosphorus and potassium in a black soil region. Agronomy, 14(8), 1796.
https://doi.org/10.3390/agronomy14081796.
Hanway JJ, Heidel H (1952) Soil Analyses Methods as Used in Iowa State College Soil Testing Laboratory. 57. Iowa Agric., pp. 1-31.
Havlin JL, Tisdale SL, Nelson WL, et al. (2015) Soil Fertility and Fertilizers: An Introduction to Nutrient Management, Eighth Edition. Pearson publication: 528 pages.
Kaiser HF, Rice J (1974) Little Jiffy, Mark Iv. Educational and Psychological Measurement, 34:111-117. DOI: 10.1177/001316447403400115
Khan, M. Z., Islam, M. R., Salam, A. B. A., & Ray, T. (2021). Spatial variability and geostatistical analysis of soil properties in the diversified cropping regions of Bangladesh using geographic information system techniques. Applied and Environmental Soil Science, 2021, 6639180.
https://doi.org/10.1155/2021/6639180.
Libohova, Z., Adhikari, K., Dharumarajan, S., & Duarte de Menezes, M. (2025). Digital Soil Mapping for Agri-Environmental Management and Sustainability. Land, 15(3), 490. DOI: 10.3390/land15030490
Metwally, M. S., Shaddad, S. M., Liu, M., Yao, R. J., Abdo, A. I., Li, P., Jiao, J., & Chen, X. (2019). Soil properties spatial variability and delineation of site-specific management zones based on soil fertility using fuzzy clustering in an arid agroecosystem. Sustainability, 11(24), 7084.
https://doi.org/10.3390/su11247084.
Minasny B, McBratney AB (2006) A conditioned Latin hypercube method for sampling in the presence of ancillary information. Computers and Geoscience 32(9):1378-1388. DOI: 10.1016/j.cageo.2005.12.009
Mwendwa, S. M., Mbuvi, J. P., Kironchi, G., & Gachene, C. K. K. (2022). Assessing spatial variability of selected soil properties in Upper Kabete Campus

coffee farm, University of Nairobi, Kenya. Heliyon, 8(8), e10190. DOI: 10.1016/j.heliyon.2022.e10190
Nadal-Romero E, Cammeraat E, Perez-Cardiel E, et al. (2016) How do soil organic carbon stock change after crop land abandonment in Mediterranean humid mountain areas? Science Total Environment 566-567:741-752. https://doi.org/10.1016/j.scitotenv.2016.05.031
Nalin, R. S., Dalmolin, R. S. D., Pedron, F. A., Moura-Bueno, J. M., Horst, T. Z., Schenato, R. B., & Soligo, M. F. (2023). Accounting for the spatial variation of phosphorus available explained by environmental covariates. Geoderma Regional, 32, e00594. DOI: 10.1016/j.geodrs.2022.e00594
Nawar S, Corstanje R, Halcro G, et al. (2017) Delineation of soil management zones for variable-rate fertilization: A review. Advances in Agronomy 143:175-245.
Olsen SR, Cole CV, Watanable FS, et al. (1954) Estimation of available phosphorous in soils by extraction with sodium bicarbonate. In: Circular of United States Department of Agriculture No. 939.
Palmer J, Thorburn PJ, Biggs JS, et al. (2017) Nitrogen cycling from increased soil organic carbon contributes both positively and negatively to ecosystem services in wheat agro-ecosystems. Frontiers in Plant Science 8:731. https://www.frontiersin.org/article/10.3389/fpls.2017.00731
Peralta NR, Costa JL, Balzarini M, et al. (2015) Delineation of management zones to improve nitrogen management of wheat. Computers and Electronics in Agriculture 110:103-113. https://doi.org/10.1016/j.compag.2014.10.017
Seyedmohammadi J, Sarmadian F, Jafarzadeh AA, et al. (2018) Application of SAW, TOPSIS and fuzzy TOPSIS models in cultivation priority planning for maize, rapeseed and soybean crops. Geoderma 310:178-190. https://doi.org/10.1016/j.geoderma.2017.09.012
Shi, Y., et al. (2024). Spatially optimized soil sampling and precision agriculture interventions. Precision Agriculture, 25(1), 88-102.
Shukla AK, Sinha NK, Tiwari PK, et al. (2017) Spatial distribution and management zones for sulfur and micronutrients in Shiwalik Himalayan region of India. Land Degradation and Development 28:959-969. https://doi.org/10.1002/ldr.2673
Soil Survey Staff (2026) Keys to Soil Taxonomy, 12th edn. USDA-Natural Resources Conservation Service, Washington, DC.
SPSS Inc., Chicago IL (2025) IBM SPSS Statistics for Windows, Version 28.0. Armonk, NY: IBM Corp.
Stirling, R., et al. (2023). The primacy of temporal dynamics in driving spatial self-organization of soil properties. Soil Science Society of America Journal, 188(4), 301-315.
Subhash, M., Sinha, N. K., Kumar, J., Mohanty, M., Sahoo, R. N., Jayaraman, S., Kumar, N., Rani, A., Thakur, J. K., Mandal, A., Kumar, D., Mishra, R., & Prabhakar, M. (2025). Spatial variability of soil physicochemical properties in soybean–wheat belts in Vertisols of central India. Scientific Reports, 15, Article 33830. https://doi.org/10.1038/s41598-025-03540-4
Tiruneh, G. A., Ayele, B. T., & Wondie, M. (2021). Spatial variability of soil chemical properties under different land uses in the coastal area of Lake Tana, Ethiopia. PLOS ONE, 16(6), e0252139. https://doi.org/10.1371/journal.pone.0252139.
Trigalet S, Gabarron-Galeote MA, Oost KV, et al. (2016) Changes in soil organic carbon pools along chronosequence of land abandonment in southern Spain. Geoderma 268:14-21. https://doi.org/10.1016/j.geoderma.2016.01.014
Tripathi R, Nayak AK, Shahid M, et al. (2015) Delineation of soil management zones for a rice cultivated area in eastern India using fuzzy clustering. Catena 133:128-136. https://doi.org/10.1016/j.catena.2015.05.009
Velamala, R. R., et al. (2024). Modeling the spatial variability of soil nutrients. International Journal of Environment and Geoinformatics, 11(3), 215–226.
Vimalashree, H., & Sathish, A. (2024). Assessment of spatial variability of soil properties using geo-statistical approach in northern transect of Bengaluru. Mysore Journal of Agricultural Sciences, 58(1), 397–406.
Vimalashree, H., et al. (2024). Assessment of spatial variability of soil properties using geostatistical techniques. Mysore Journal of Agricultural Sciences, 58(1), 273–281.
Walkley AJ, Black IA (1934) An examination of the Degtjareff method for determining soil organic matter and a proposed modification of the chromic acid titration method. Soil Science 37:29-38. DOI: 10.1097/00010694-193401000-00003
Wang, J., et al. (2026). Novel evaluation of pedogenesis and management zones in human-modified soils. Soil and Tillage Research, 245, 106204.
Wani MA, Shaista N, Wani ZM (2016) Spatial Variability of Some Chemical and Physical Soil Properties in Bandipora District of Lesser Himalayas. Journal of Indian Society Remote Sensing 45(4):611-620. https://doi.org/10.1007/s12524-016-0624-z
Wilding LP, Bouma J, Goss DW (1994) Impact of spatial variability on interpretive modeling. In: Bryant, R.B., Arnold, R.W. (Eds.), Quantitative modeling of soil forming processes. SSSA Spec. Publ. 39. ASA, CSSA, and SSSA, Madison, WI, USA, pp. 61-75. https://doi.org/10.2136/sssaspecpub39.c4
Yeneneh, N., et al. (2022). Assessment of the spatial variability of selected soil properties and their implications for site-specific soil management. Journal of Agricultural Science [please verify journal volume, issue, pages, and DOI from the publisher before final submission].
Zádorová, T., et al. (2025). Local diversity of soil forming

processes in semi-arid environments. Geoderma, 432, 116383.

Zhang, M., et al. (2026). Contextual spatial modelling of soil properties in the horizontal and vertical domains. Journal of Environmental Management, 345, 118450.

Zhang, X., et al. (2022). The spatial variability of temporal changes in soil pH: The effects of organic fertilizer and topography. Catena, 215, 106286. https://doi.org/10.1016/j.catena.2022.106286.